

Design of Path Planning Controller of Autonomous Wheeled Mobile Robot Based on Triple Pendulum Behaviour

Salah M. Swadi*, Ahmed K. Kadhim, and Ghusoon M. Ali

Electrical Engineering Department, College of Engineering, Munstansiriyah University, Baghdad, Iraq

Email: {s.m.swadi, a.k.kadhim, eng.ghusoon_ali}@uomustansiriyah.edu.iq

*Correspondence: s.m.swadi@uomustansiriyah.edu.iq

Abstract—This paper deals with the path planning of autonomous differential driving wheeled mobile robots. The path planning controller of the mobile robot is designed based on the chaotic behaviour of the Triple Pendulum (TP). The dynamic response of the TP is investigated using Simscape Multibody software. The chaotic behaviour of the TP is examined with a 0-1 test. The proposed model was tested with five different scenarios. In each experiment, the robot is designed to search for a target that may represent an exit point, dangerous material, or any specific target. This target is placed in an arbitrary position on a square arena 2500 mm by 2500 mm. In order to increase the complexity of the robot mission, the target is surrounded by an obstacle (u-shape) so that there is a unique entrance for the robot to reach the target. In addition, the proposed controller is compared with the controller based on a traditional chaotic system (Lorenz system), which is designed for this purpose. In this work, simulation results are conducted using the KiKS simulator. The results show the success of the proposed controller in completing all missions with 13.11 sec, 17.09 sec, 36.47 sec, 12.52 sec, and 12.49 sec for scenarios 1, 2, 3, 4, and 5, respectively. The second controller completed the same mission in 25.22 sec, 32.28 sec, 46.49 sec, 49.4 sec, and 33.38 sec. These results proved the proposed controller's advantage, which has great potential and can be investigated in the future.

Keywords—wheeled mobile robot, path planning, triple pendulum, Lorenz system, 0-1 test, chaotic systems

I. INTRODUCTION

The first chaotic system is presented by Lorenz, which has three first-order Ordinary Differential Equations (ODEs), during the study of the atmospheric convection [1]. This phenomenon has great potential in many fields. Following Lorenz, many researchers try to discover new formulas for the chaotic system or new applications for such a system. In this work, the chaotic behaviour of a trip pendulum is combined with a mobile robot. This is accomplished by designing a mobile robot controller based on that behaviour for the path-planning problem of

mobile robots. This strategy ensures fast scanning of an unknown environment for searching purposes.

Nakamura and Sekiguchi employ chaotic behaviour in the mobile robot. They design a mobile robot controller based on Arnold's chaotic system, which generates a chaotic trajectory. One variable of the Arnold system is selected to control the angular velocity of the mobile robot and maintain the robot to move in constant linear velocity [2]. Petavratzis et al. [3] reported on the May maps chaotic system to represent robot path arrangement that had a discrete movement of 4 and 8 directions. Others reported that chaotic changing aspects drive mobile wheel robot for path planning to provide self-directed navigation [4]. Mobile robots with dynamic workspace covering algorithms could be uncertain to predicate or guarantee the entire area. The reason behind that is the chaos's natural properties, including the dense orbits, topological transitivity, and initial condition sensitivity [5]. In addition, applying an autonomous navigation technique to utilise chaotic control signals for wheeled robots required fewer programming efforts, hardware resources, and algorithms.

The Arduino-embedded platform would be enough to build and design a prototype of that system [6]. However, in terms of energy efficiency, the method is considered to be promising. A novel hyperjerk chaotic system is proposed by L. Moysis et al. [7]. This system is four-dimension with only one nonlinear term (hyperbolic sine). Using a combination of a modulotactic and sampling technique, the suggested system is applied as a chaotic producer to pass the problem of a chaotic path. In [8], the logistic map chaotic system is used as a path-planning controller for mobile robots to move in the workspace. Recently, [9] an unpredictable velocity profile for the quadrotor has been designed based on chaotic systems. The mirror mapping approach has been used to keep the quadrotor within the objective area. As well as, nonlinear velocity and attitude control laws have been proposed to guarantee velocity tracking.

Fast scanning of the workspace is required to find a specific target placed in an arbitrary location of an unmapped area. Path planning based on the chaotic behaviour of the dynamic system can be an excellent

solution to achieve this task. The main characteristics of the chaotic system are topological transitivity and the sensitive dependence on initial conditions [1].

In this paper, TP behaviour is implemented to design an autonomous mobile robot controller, unlike the traditional method mentioned previously. In addition, the comparison is made between the proposed system and the commonly used chaotic system (Lorenz system)

II. METHODOLOGY

A. Dynamic Model of TP

In classical mechanics and chaos studies, Double and TPs are examined, although they are not commonly a traditional problem in physics areas. For instance, Lagrange Mechanics is used to obtain the behaviour equations of these systems, which are complicated and lengthy. The equations themselves could be solved using ordinary derivations. These equations would involve complex tasks which may arise in computer CPUs. However, the existence of partial systems containing more than three point masses or any higher-order systems.

Consequently, reducing the time of calculating in these systems could be achieved using the new formulation of equations for n-points masses pendulum, hence, helping with chaos studying in those systems. The pendulum system investigated in this paper consists of point masses and movable joints [10]. Fig. 1 shows the configuration of the TP, which is investigated in this paper.

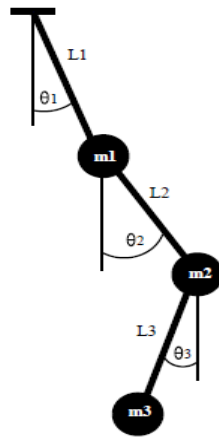


Figure 1. Triple pendulum model

The Lagrangian of the TP can be written as $L = L_1 + L_2 + L_3$. The equation of motion of TP can be written concerning θ_1 , θ_2 and θ_3 using the Euler-Lagrange Eq. (1),

$$\frac{d}{dt} \left(\frac{\partial L}{\partial \dot{q}} - \frac{\partial L}{\partial q} \right) = 0 \quad (1)$$

For θ_1

$$gL_1(m_1 \sin(\theta_1) + m_2 \sin(\theta_1) + m_3 \sin(\theta_1)) + m_2 L_1 L_2 \sin(\theta_1 - \theta_2) \dot{\theta}_1 \dot{\theta}_2 + m_3 L_1 L_3 \sin(\theta_3 - \theta_1) (\dot{\theta}_1 - \dot{\theta}_3) + m_3 L_1 L_2 \sin(\theta_1 - \theta_2) \dot{\theta}_1 \dot{\theta}_2 + L_1^2 \dot{\theta}_1 (m_1 + m_2 + m_3) + m_2 L_1 L_2 [\sin(\theta_2 - \theta_1) (\dot{\theta}_1 - \dot{\theta}_2) \dot{\theta}_2 + \cos(\theta_1 - \theta_2) \ddot{\theta}_2] + m_3 L_1 L_2 [\sin(\theta_2 - \theta_1) (\dot{\theta}_1 - \dot{\theta}_2) \dot{\theta}_2 + \cos(\theta_1 - \theta_2) \ddot{\theta}_2] + m_3 L_1 L_3 [\sin(\theta_3 - \theta_1) (\dot{\theta}_1 - \dot{\theta}_3) \dot{\theta}_3 + \cos(\theta_1 - \theta_3) \ddot{\theta}_3] = 0 \quad (2)$$

For θ_2

$$gL_2(m_2 \sin(\theta_2) + m_3 \sin(\theta_3)) + \dot{\theta}_1 \dot{\theta}_2 L_1 L_2 \sin(\theta_2 - \theta_1) (m_1 + m_2) + m_3 L_2 L_3 \sin(\theta_2 - \theta_3) (\dot{\theta}_2 \dot{\theta}_3) + L_2^2 \ddot{\theta}_2 (m_2 + m_3) + (m_2 + m_3) L_1 L_2 [\sin(\theta_2 - \theta_1) (\dot{\theta}_1 - \dot{\theta}_2) \dot{\theta}_1 + \cos(\theta_2 - \theta_1) \ddot{\theta}_1] + m_3 L_2 L_3 [\sin(\theta_3 - \theta_2) (\dot{\theta}_2 - \dot{\theta}_3) \dot{\theta}_3 + \cos(\theta_3 - \theta_2) \ddot{\theta}_3] = 0 \quad (3)$$

For θ_3

$$m_3 g L_3 \sin(\theta_3) - m_3 L_2 L_3 \sin(\theta_2 - \theta_3) \dot{\theta}_2 \dot{\theta}_3 - m_3 L_1 L_3 \sin(\theta_1 - \theta_3) \dot{\theta}_1 \dot{\theta}_3 + m_3 L_1 L_3 [\sin(\theta_3 - \theta_1) (\dot{\theta}_1 - \dot{\theta}_3) \dot{\theta}_1 + \cos(\theta_1 - \theta_3) \ddot{\theta}_1] + m_3 L_2 L_3 [\sin(\theta_3 - \theta_2) (\dot{\theta}_2 - \dot{\theta}_3) \dot{\theta}_2 + \cos(\theta_2 - \theta_3) \ddot{\theta}_2] + m_3 L_2^2 \ddot{\theta}_3 = 0 \quad (4)$$

B. TP Design Using Simscape Multibody Software

Due to the complexity of the dynamic model of the TP, as presented in section A, numerical techniques are often used to estimate the dynamic behaviour of the system. Here, a simpler, faster, and more accurate alternative method is presented. The TP is analysed using Simscape Multibody software.

Simscape Multibody (or SimMechanic) provides a simulation environment for 3D mechanical systems (usually consisting of multibody). These systems can be as complicated as aircraft landing gear, robots, hydraulic systems, and vehicle suspension systems [11].

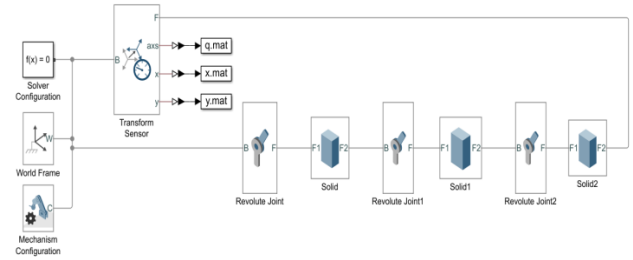


Figure 2. Simulink model of TP

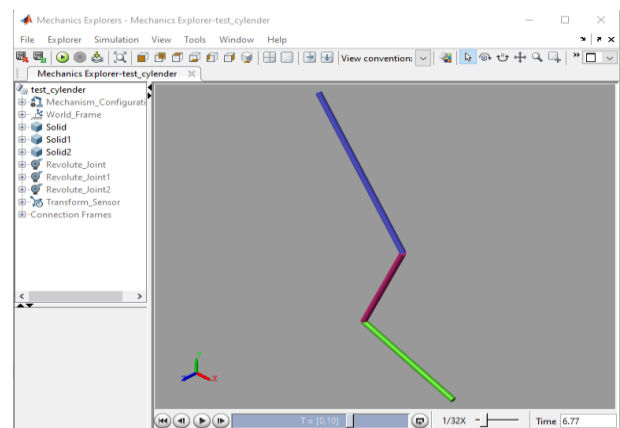


Figure 3. Virtual Simulink model of TP

SimMechanic provides a variety of blocks to modelled multibody systems that represent masses and joints, in addition to constraints, force elements, and represent sensors. The significant feature of SimMechanic is the ability to solve the equation of motion of a complicated mechanical system. It can estimate the accurate value of mechanical system inertia, which is considered an important and challenging issue

for researchers. Simscape Multibody has an important feature: the ability to import the model built using a CAD package, including all important information inertia, constraints, masses, and system geometry. Visualising system dynamics (3D animation) helps researchers to develop their models. Control systems can be conducted using a SimMechanics environment and test model behaviour. The system model parametrised by MATLAB to design the control system of the multibody can be implemented in Simulink.

Many sub-systems, such as electrical, pneumatic, and hydraulic, can be integrated into a model utilising the Simscap components. In addition, the designed models can be deployed to hardware that supports C-code generation [11]. Figs. 2 and 3 show the Simulink and virtual model of the TP, which were built using the Simscape Multibody software. The proposed model mainly consists of links (Link1, Link2, and Link3) and revolute joints (Revolute Joint, RevoluteJoint1, and Revolute Joint2). An important block is the Transform Sensor, which permits to measure of many essential variables such as position (x, y, and z), and angular velocity frames about (x-, y- and z-) axes regarding the reference frame (world frame).

C. Chaotic Behaviour of TP

The chaotic behaviour of any dynamic system can be investigated using different approaches. In this paper, time series, random (chaotic) trajectory, and 0-1 test are considered to find the chaotic behaviour of the TP. The parameters of the TP are ($m_1=18$ kg, $m_2=6.28$ kg, $m_3=3.14$ kg, $L_1=0.3$ m, $L_2=L_3=0.2$ m). Figs. 4 to 6 show the time series of the x-coordinate, y-coordinate and origin angular velocity for the last frame. These figures exhibit a random or at least not predictable response of the system, but actually, it conducts from a deterministic system (i.e., equations 2, 3, and 4). It is an important sign of a chaotic system. Fig. 7 shows the trajectory of the same last frame in the (x-y) plane. The trajectory in the phase plane is quickly attracted to a small region. These results are typical for a non-periodic response (i.e., similar to the results of the Lorenz system in section C).

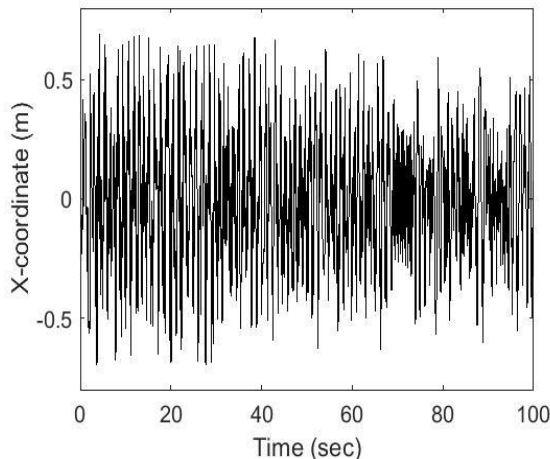


Figure 4. Time series of x-coordinate of the TP free end

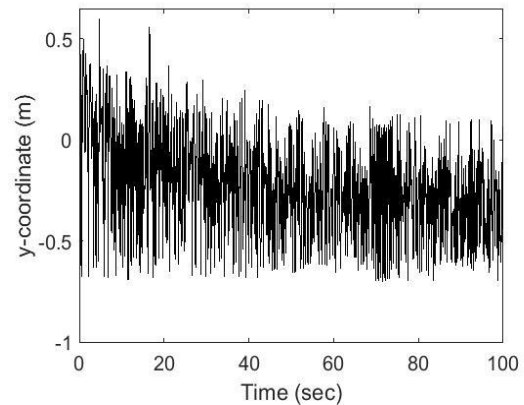


Figure 5. Time series of y-coordinate of the TP free end

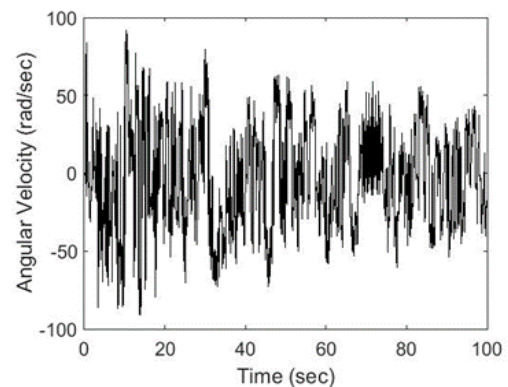


Figure 6. Time series of the angular velocity of the TP free end

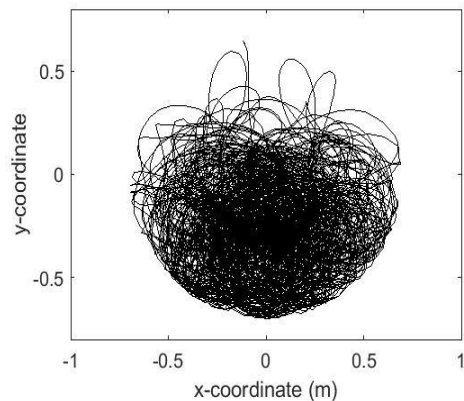


Figure 7. The trajectory of the TP-free end

1) The (0-1) Test

Many research efforts have been made to develop the 0-1 test [12-14]. This test is used to clarify chaotic dynamics in a dynamic system. Despite the standard Lyapunov exponent method requiring phase space reconstruction to analyse the dynamics system response, 0-1 test analysis of the time series without data preprocessing. Furthermore, the minimal computational effort is required for the 0-1 test, independent of the dynamic system dimension under investigation. $\emptyset(n)$ is a discrete data set, sampled at times $n = 1, 2, 3$. This set denotes a 1D obvious data set. The following can be defined by choosing a constant $c \in \mathbb{R}^+$ at random [15].

$$p(n) = \sum_{j=1}^n \phi(j) \cos(\theta(j)), \quad n = 1,2,3.. \quad (5)$$

$$q(n) = \sum_{j=1}^n \phi(j) \sin(\theta(j)), \quad n = 1,2,3.. \quad (6)$$

Where

$$\theta(j) = jc + \sum_{j=1}^n \phi(j), \quad j = 1,2,3, \dots, n \quad (7)$$

Then, by using $p(n)$ (alternatively $s(n)$), the mean square displacement can be defined as:

$$N(n) = \lim_{N \rightarrow \infty} \frac{1}{N} \sum_{j=1}^n [p(j+n) - p(j)]^2, n=1,2,3.. \quad (8)$$

The Brownian behaviour happens when $p(n)$ and $s(n)$ have the same response, and then $M(n)$ raises linearly with time. When $p(n)$ is bounded, $M(n)$ is also bounded. (9) define the asymptotic growth rate

$$K = \lim_{n \rightarrow \infty} \frac{\log M(n)}{\log n} \quad (9)$$

The value of K distinguishes between regular and chaotic systems, where when $K=0$, that is for a regular system, and when $K=1$, that is for a chaotic system.

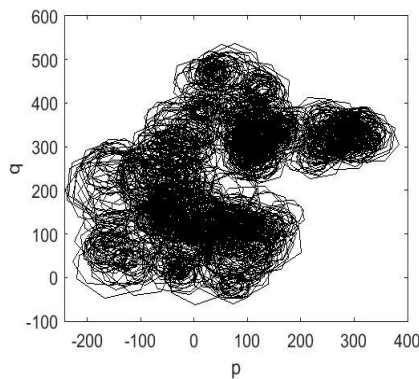


Figure 8. Dynamics of the translation components (p, q) of the triple pendulum

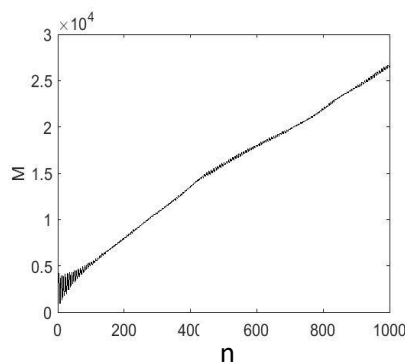


Figure 9. The mean square displacement M versus n for the triple pendulum

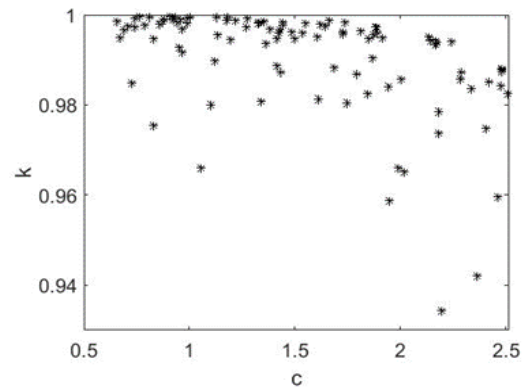


Figure 10. K versus c for the triple pendulum ($K_{\text{median}} = 0.9942$)

Now, apply the 0-1 test on the time series of the angular velocity of the last frame. Fig. 8 shows the dynamics of the translation components p and q for the time series of the angular velocity of the last frame of the TP. While Fig. 9 shows the mean square displacement M versus n , both figures indicate chaotic behaviour. Finally, Fig. 10 shows K versus c for the TP. It is clearly stated that the pendulum response is chaotic, where $K(\text{median})$ is equal to 0.9942.

2) Lorenz system

Another chaotic controller using the Lorenz system is built to compare the efficiency of the chaotic controller based on the TP behaviour. Consequent to the 3D Lorenz system invention, many chaotic systems were invented. Many investigations into applications of chaos systems, for example, secure communications, synchronisation, motion control, and improved algorithms [16, 17 and 18]. The differential equations of the Lorenz system are as follows:

$$\begin{aligned} \dot{x} &= \sigma(y - x) \\ \dot{y} &= rx - y - xz \\ \dot{z} &= xy - bz \end{aligned} \quad (10)$$

Where:

$$\sigma = 10, \quad r = 28, \quad b = 8/3$$

The time series and the strange attractor are shown in Figs. 11 and 12, respectively [19]. These figures show the typical behaviour of aperiodic dynamic systems. Since the Lorenz system is well-known as a chaotic system, an important conclusion can be made by comparing these results with the TP response shown in Figs. 4, 5, and 7 confirm that both systems have chaotic properties.

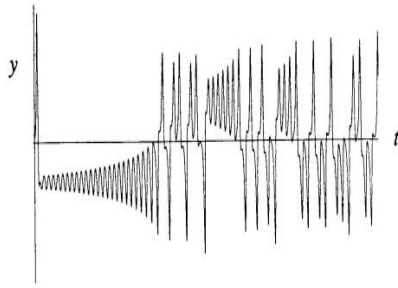


Figure 11. Time series of Lorenz system.

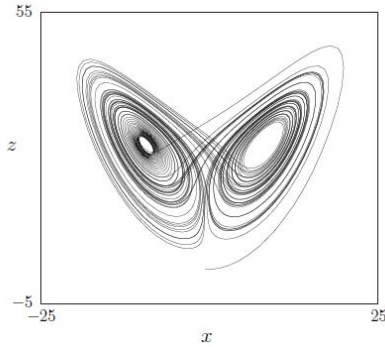


Figure 12. The 2-D strange attractor of Lorenz system

D. Dynamic Model of the Mobile Robot

The Differential Driving Wheeled Mobile Robot (DDWMR) consists of two active, driven wheels and a passive caster wheel, which can be added for robot stability. Additional stability can be achieved when the castor wheel is positioned in the front/rear of the robot chassis. Due to its simplicity and stability, the DDWMR is the typical design deployed for indoor mobile robots.

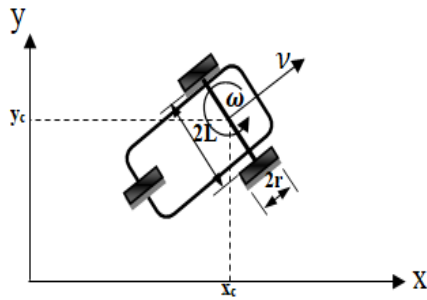


Figure 13. Nonholonomic mobile robot platform

Kinematics studies motion without force effectiveness. Referring to Fig. 13, the kinematic equation of the mobile robot in world frame $\{o, x, y\}$ can be expressed as follows [20]:

$$\dot{x}_c(t) = v(t)\cos\theta(t) \quad (11)$$

$$\dot{y}_c(t) = v(t)\sin\theta(t) \quad (12)$$

$$\dot{\theta}(t) = \omega(t) \quad (13)$$

The kinematic (11), (12), and (13) can be represented in matrix form as follows:

$$\begin{bmatrix} \dot{x}_c \\ \dot{y}_c \\ \dot{\theta} \end{bmatrix} = \begin{bmatrix} \cos\theta & 0 \\ \sin\theta & 0 \\ 0 & 1 \end{bmatrix} \begin{bmatrix} v \\ \omega \end{bmatrix} \quad (14)$$

Where:

v = the linear velocity of the mobile robot (m/s).

ω = the angular velocity of the mobile robot (rad/s).

1) Mobile robot controller design

To integrate the chaotic behaviour of the TP into a mobile robot, the angular velocity of the third link (time series in Fig. 6) is chosen to control the mobile robot's direction.

$$\begin{bmatrix} \dot{x}_c \\ \dot{y}_c \\ \dot{\theta} \end{bmatrix} = \begin{bmatrix} \cos\theta & 0 \\ \sin\theta & 0 \\ 0 & 1 \end{bmatrix} \begin{bmatrix} v \\ \dot{\theta} \end{bmatrix} \quad (15)$$

Where:

$\dot{\theta}$ = the angular velocity of the third link of TP (rad/sec).

To integrate the chaotic behaviour of the Lorenz system into the mobile robot, (16) can be used:

$$\begin{bmatrix} \dot{x} \\ \dot{y} \\ \dot{z} \\ \dot{x}_c \\ \dot{y}_c \end{bmatrix} = \begin{bmatrix} \sigma(y-x) \\ rx-y-xz \\ xy-bz \\ v\cos z \\ v\sin z \end{bmatrix} \quad (16)$$

The system, as expressed in (16), includes the chaotic system and the kinematic equation of the MR, where the robot is assumed to move at a constant velocity and be steered according to one variable chosen from the chaotic system (Here, z variable is chosen).

2) Khepera simulator (KiKS)

The simulation program considered in this paper to conduct the control strategy is performed using the KiKS Simulator. The KiKS Simulator is a Matlab program that simulates a Khepera (II) robot connected to a computer similar to the actual Kheperas. The robot consists of two wheels and eight proximity sensors. The velocity and wheels turning are controlled. The sensors deliver short-range obstacle distance data. This model is shown in Fig. 14, six sensors are placed on the front side, and two others are on the back side to allow back manoeuvring. These sensors allow the robot to detect obstacles and workspace boundaries. When the robot goes into boundaries, it takes a reflexive trajectory that requires the measurement of the local normal to the obstacle when the sensors sense the closeness of the obstacle [20].

III. SIMULATION RESULTS AND DISCUSSION

The control strategy is tested using the Khepera robot simulator. The simulation program is designed in such a manner as to make a robot search for a waypoint (target) in an unmaped arena. To make a comparison between

both mobile robot controllers (i.e. designed in section D), different scenarios are considered as follows:

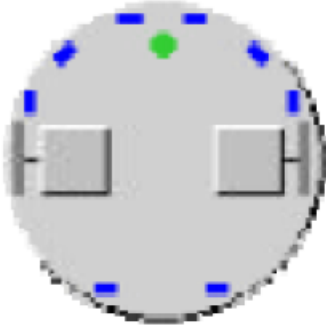


Figure 14. the simulated KHEPERA mobile robot.

1) Scenario 1

In this scenario, the waypoint is placed below the centre point of the area, and the robot starts moving from the centre point as in all scenarios with linear velocity =0.3 m/s and integrated step $h=0.1$. Fig. 15 shows the trajectory of the mobile robot, which is generated from the Lorenz system. It takes about 25.22 sec to complete the task. The system's initial position is $x(1)=1$, $y(1)=0$, and $z(1)=1$. Fig. 16 shows the trajectory of the mobile robot, which is produced according to the chaotic behaviour of TP, and the robot takes only 13.11 sec to find the waypoint. The initial angle of the TP is $\theta_1 = 80^\circ$, $\theta_2 = -20^\circ$, and $\theta_3 = -30^\circ$ (with respect to the y-axis).

2) Scenario 2

If the target is placed in the upper right corner of the area, it is expected to take more time for the robot to find the target due to the complexity of this task. Fig. 17 shows the trajectory of the chaotic mobile robot, which uses the Lorenz system, where it takes about 32.28 sec to find the target. The system initial position for this case is $x(1)=10$, $y(1)=5$, and $z(1)=4$. While it takes only 17.09 sec to complete the same task by the robot that uses the TP behaviour as shown in Fig. 18. The initial angle of the TP is $\theta_1 = 85^\circ$, $\theta_2 = -15^\circ$, and $\theta_3 = -25^\circ$.

3) Scenario 3

This scenario deals with the target placed in the area's upper left corner. It is opposite to the position in Scenario 2. Fig. 19 shows the trajectory of the chaotic mobile robot, which uses the Lorenz system, where it takes about 46.49 sec to find the target. The system's initial position for this case is $x(1)=5$, $y(1)=10$, and $z(1)=-3$. While it takes only 36.47 sec to complete the same task by the robot that uses the TP behaviour as shown in Fig. 20. The initial angle of the TP is $\theta_1 = -75^\circ$, $\theta_2 = -10^\circ$, and $\theta_3 = -20^\circ$.

4) Scenario 4

Where the target is placed in the lower-left corner of the area, Fig. 21 shows the trajectory of the chaotic mobile robot, which uses the Lorenz system, where it takes about 49.11 sec to find the target. The system initial

position for this case is $x(1)=2$, $y(1)=2$, and $z(1)=2$. While it takes only 12.52 sec to complete the same task by the robot that uses the TP behaviour as shown in Fig. 22. The initial angle of the TP is $\theta_1 = 70^\circ$, $\theta_2 = -7^\circ$ and $\theta_3 = -5^\circ$.

5) Scenario 5

Here, the target is placed in the lower-left corner of the area. It is the opposite of the position in scenario 4. The system initial position for this case is $x(1)=-1$, $y(1)=-1$, and $z(1)=-1$. Fig. 23 shows the trajectory of the chaotic mobile robot, which uses the Lorenz system, where it takes about 33.38 sec to find the target. While it takes only 12.49 sec to complete the same task by the robot that uses the Triple Pendulum behaviour as shown in Fig. 24. The initial angle of the TP is $\theta_1 = 60^\circ$, $\theta_2 = -17^\circ$, and $\theta_3 = 7^\circ$,

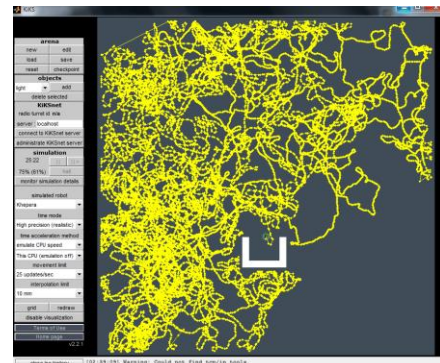


Figure 15. Mobile robot trajectory Lorenz system based, Simulation time 25.22 (sec).

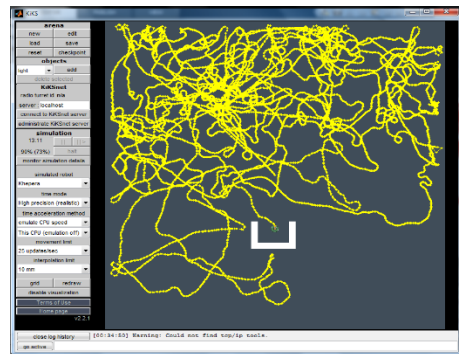


Figure 16. Mobile robot trajectory TP-based, simulation time 13.11 (sec).

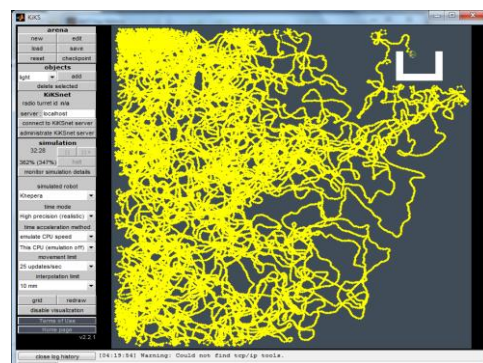


Figure 17. Mobile robot trajectory Lorenz system based, simulation time 32.28 (sec).

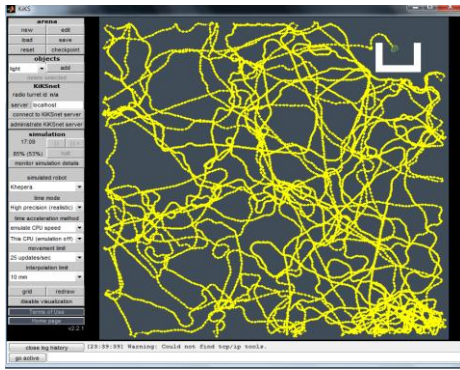


Figure 18. Mobile robot trajectory TP-based, simulation time 17.09 (sec).

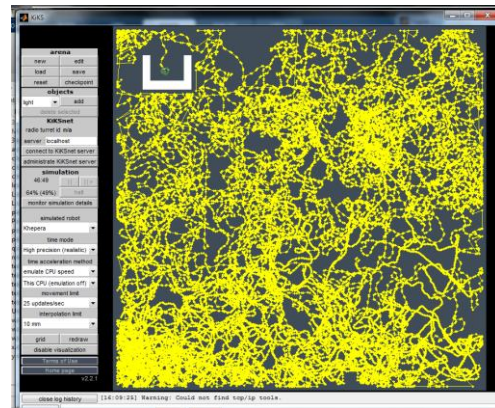


Figure 22. Mobile robot TP-based, simulation time 12.52 (sec).

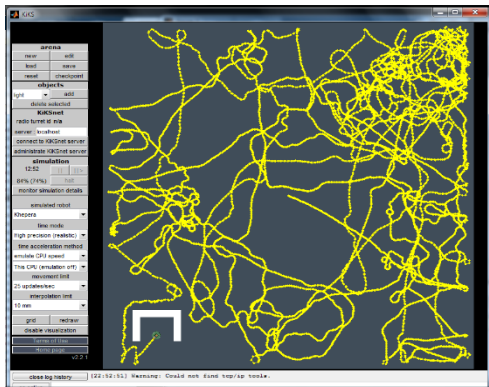


Figure 19. Mobile robot trajectory Lorenz system based, simulation time 46.49 (sec).

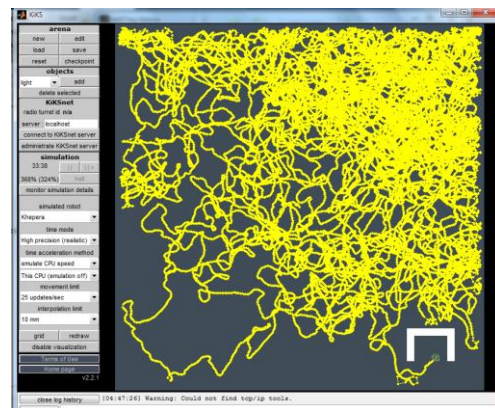


Figure 23. Mobile robot trajectory Lorenz system based, simulation time 33.38 (sec).

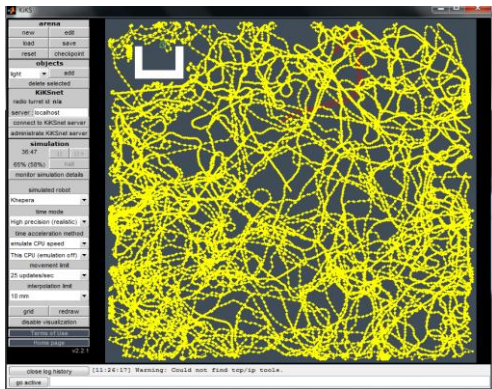


Figure 20. Mobile robot trajectory TP-based, simulation time 36.47 (sec).

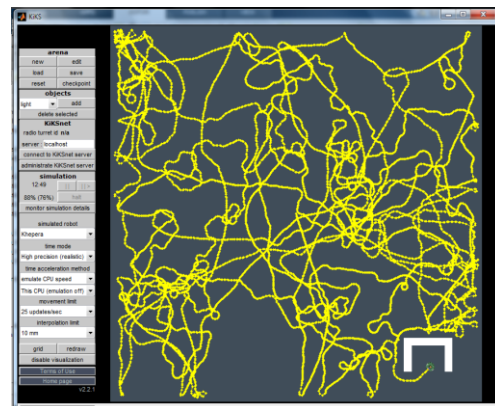


Figure 24. Mobile robot trajectory TP-based, simulation time 12.49 (sec).

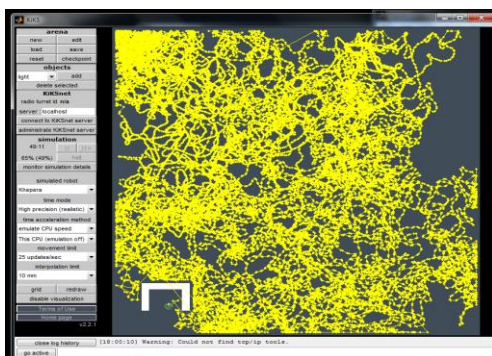


Figure 21. Mobile robot trajectory Lorenz system based, simulation time 49.11 (sec).

From above, both controllers successfully complete all missions despite the complexity of the unmapped area and the presence of an obstacle. The initial conditions of both controllers have been changed in each scenario to avoid repeating the same trajectory in all missions, which causes fogging in evaluation. Furthermore, simulation results showed the usefulness of the proposed controller (based on TP behaviour) in such applications where it was faster than the Lorenz based. The time average of all scenarios was 18.34 sec for the controller based on TP and 37.3 sec for the second controller. Table I presents the summary of simulation time for each scenario and

both controllers. The progress of mobile robot TP is based on Lorenz in all scenarios.

IV. CONCLUSION

In this paper, a path planning controller based on the chaotic behaviour of the TP is presented. The dynamic model of TP is presented. Due to the complexity of the dynamic module of TP and higher order, an alternating method has been used. Dynamic response of TP is conducted with Simscap Multibody software such as time series of x –coordinate, y-coordinate, and angular velocity of the end of the 3rd link. The 0-1 test of the angular velocity of the 3rd link shows the chaotic behaviour of the TP. According to the time series of the angular velocity, a path-planning controller for mobile robots is designed. To validate the efficiency of the proposed controller, a comparison has been made with another controller based on the Lorenz system. Both controllers were evaluated throughout the test program. This program is composed of 6 scenarios. In each task, the robot must find a target placed arbitrarily in an unmapped area of 2500 mm × 2500 mm. In order to increase the challenge of the tasks, the target is surrounded by an obstacle of a u-shape, so there is a unique entrance for the robot to reach the target.

Simulation results show that both controllers succeeded in completing their mission. The proposed robot controller based on TP behaviour is faster than the robot controller based on a traditional chaotic system (i.e. Lorenz system) which saves time by about 50%. The chaotic behaviour of the TP has excellent potential in such applications, which may be investigated in the future. Simscap Multibody software can be reduced to overcome the difficulties of analysing a complex dynamic system with sufficient accuracy. KiKS simulator is a beneficial program for a mobile robot with many tools integrated with Matlab software.

TABLE I. SIMULATION TIME AND INITIAL POSITION FOR BOTH CONTROLLER

Scenario No.	Simulation time of Lorenz-based (sec)	Simulation time of TP-based (sec)	The initial position of the Lorenz system	The initial position of TP
1	25.22	13.11	x(1) = 1 y(1) = 1 z(1) = 1	$\theta_1 = 0^\circ$ $\theta_2 = -20^\circ$ $\theta_3 = -30^\circ$
2	32.28	17.09	x(1) = 10 y(1) = 5 z(1) = 4	$\theta_1 = 85^\circ$ $\theta_2 = -15^\circ$ $\theta_3 = -25^\circ$
3	46.49	36.47	x(1) = 5 y(1) = 10 z(1) = -3	$\theta_1 = -75^\circ$ $\theta_2 = -10^\circ$ $\theta_3 = -20^\circ$
4	49.11	12.52	x(1) = 2 y(1) = 2 z(1) = 2	$\theta_1 = 70^\circ$ $\theta_2 = -7^\circ$ $\theta_3 = -5^\circ$
5	33.38	12.49	x(1) = -1 y(1) = -1 z(1) = -1	$\theta_1 = 60^\circ$ $\theta_2 = -17^\circ$ $\theta_3 = -7^\circ$

CONFLICT OF INTEREST

The authors declare no conflict of interest

AUTHOR CONTRIBUTIONS

Salah M. Swadi investigated the opportunity of using triple pendulum behavior in path planning strategy, and he designed the mobile robot controller that is based on triple pendulum behavior (methodology).

Ahmed K. Kadhim designed the Simulink model of the triple pendulum, and evaluated simulation results. He also wrote, reviewed and edited the manuscript.

Ghusson M. Ali supervised and managed the work. He analyzed the data, reviewed and edited the manuscript.

Finally, all authors had approved the final version.

ACKNOWLEDGEMENT

Authors thanks the Mustansiriyah University (www.uomustansiriyah.edu.iq), Baghdad-Iraq, for its support in the present work.

REFERENCES

- [1] E. N. Lorenz, "Deterministic non-periodic flow," *J. Atmos. Sci.*, vol. 20, no. 1, pp. 130-141, 1963.
- [2] Y. Nakamura and A. Sekiguchi, "The chaotic mobile robot," *IEEE Transactions on Robotics and Automation*, vol. 17, no. 6, pp. 898-904, 2001.
- [3] E. Petavratzis, L. Moysis, and C. Volos, "Chaotic path planning for grid coverage using a modified logistic-may map," *Journal of Automation, Mobile Robotics and Intelligent Systems*, vol. 14, no. 2, 2020.
- [4] L. Moysis, E. Petavratzis, and C. Volos, "A chaotic path planning generator based on logistic map and modulo tactics," *Robotics and Autonomous Systems*, vol. 124, p. 103377, 2020.
- [5] M. A. Tawfik, E. N. Abdulwabb, and S. M. Swadi, "A specific chaotic system and its implementation in robotic field," *Eng. &Tech. Journal*, vol. 33, Part (A), no. 9, 2015.
- [6] C. K. Volos, I. M. Kyprianidis, and I. N. Stouboulos, "Experimental investigation on coverage performance of a chaotic autonomous mobile robot," *Robotics and Autonomous Systems*, vol. 61, no.12, p. 1314–1322, 2013.
- [7] L. Moysis, et al., "Analysis, synchronisation, and robotic application of a modified hyperjerk chaotic system," *Hindwai Complexity*, vol. 2020, April 2020.
- [8] E. Petavratzis, et. al., "An inverse pheromone approach in a chaotic mobile robot's path planning based on a modified logistic map," *Technologies*, vol. 7, no. 84, 2019.
- [9] C. Montañez-Molina, J. Pliego-Jiménez, and C. Cruz-Hernández, "Chaotic velocity profile for surveillance tasks using a quadrotor," in *Proc. of the 2021 IEEE Conf. on Control Technology and Applications (CCTA)*, San Diego, CA, USA, 9–11 August 2021.
- [10] B. Ye_silyurt, "Equations of motion formulation of a pendulum containing N-point masses," *arXiv:1910.12610v2 [physics.class-ph]*, Feb 2020.
- [11] Mathworks, Simscap Multibody Model and simulate multibody mechanical systems, [Online]. Available: <https://www.mathworks.com/products/simscap-multibody.html>.
- [12] G. A. Gottwald and I. Melbourne, "A new test for chaos in deterministic systems," in *Proc. of the Royal Soccity A.*, vol. 460, no. 2024, pp. 603–61, 2004.
- [13] G. A. Gottwald and I. Melbourne, "Testing for chaos in dnietermistic systems with noise," *Physica D: Nonlinear Phenomena*, vol. 212, no. 1-2, pp. 100–110, 2005.
- [14] G. A. Gottwald and I. Melbourne, "On the implementation of the 0–1 test for chaos," *SIAM Journal on Applied Dynamical Systems*, vol. 8, no. 1, p. 129-145, 2009.
- [15] S. Ke-Hui, L. Xuan, and Z. Cong-Xu, "The 0-1 test algorithm for chaos and its applications," *Chin. Phys. B*, vol. 19, no. 11, 2010.

- [16] G. Lindfield and J. Penny, *Numerical Methods Using MATLAB*, Fourth Edition, ScienceDirect, 2019.
- [17] A. Dinu and M. Frunzete, "The Lorenz chaotic system, statistical independence and sampling frequency," *International Symposium on Signals, Circuits and Systems (ISSCS)*.
- [18] S. Alam and P. Ahmed, "Several chaotic analysis of Lorenz system," *European Scientific Journal*, vol. 13, no. 9, 2017.
- [19] H. Broer and F. Takens, *Dynamical System and Chaos*, First edition, Groningen-Springer, 2009.
- [20] J. J. Cetina-Denis, et. al., "Design of a chaotic trajectory generator algorithm for mobile robots," *Appl. Sci.*, vol. 12, no.2587, 2022.

Copyright © 2023 by the authors. This is an open access article distributed under the Creative Commons Attribution License (CC BY-NC-ND 4.0), which permits use, distribution and reproduction in any medium, provided that the article is properly cited, the use is non-commercial and no modifications or adaptations are made.



Salah M. Swadi received the B.Eng. degree in mechanical engineering and teaching from the University of Technology, Baghdad, Iraq, in 1999, and the master's degree in mechanical engineering and the Ph.D. degree in mechanical engineering from the University of Technology, Baghdad, Iraq, in 2002 and 2016, respectively. He is currently a Lecturer in Department of Electrical Engineering, Mustansiriyah University. His current research interests include mobile robot, robotic arm, nonlinear dynamics system, control, and IoT technology. He can be contacted at email: s.m.swadi@uomustansiriyah.edu.iq



Ahmed Khalid Kadhim was born in Baghdad, Iraq, in 1987. He received the B.E. degree in electrical engineering from the University of Mustansiriyah, Baghdad, Iraq, in 2009, and the M.Sc. degrees in microelectronic engineering from the Newcastle University, UK, in 2016. In 2012, he joined the Department of Electrical Engineering, University of Mustansiriyah, as a demonstrator in the electronic laboratory, and in 2016 became a Lecturer. His current research interests include μ systems, embedded systems, and processors, internet of things (IoT), cloud computing, sensors, robotics design.



Ghusoon M. Ali received the B. Eng. (Tech.) and M. Eng. (Tech.) degrees in electrical engineering from University of Technology, Baghdad-Iraq, in 1984 and 1989, respectively, and the Ph.D. degree in electronics engineering from the Indian Institute of Technology (IIT), Banaras Hindu University, Varanasi India, in 2011. She is working as Prof. with the Electrical Engineering Department, College of Engineering, Mustansiriyah University, Baghdad-Iraq. She has published 42 research papers in leading technical journals and in Conference Proceedings. She has also worked as a principal investigator in many sponsored projects. She is a recipient of Iraq-Science-Fellowship-Program (ISFP) at Coastal Carolina University, SC, USA. Her research interests include electronic and optoelectronic devices and systems. She can be contacted at email: eng.ghusoon_ali@uomustansiriyah.edu.iq